*Int. J. Heat Mass Transfer.* Vol. 31, No. 10, pp. 1983–1991, 1988
Printed in Great Britain

0017-9310/88 $3.00+0.00


# Thermal effectiveness of multipass plate exchangers

ALBERTO PIGNOTTI and PABLO I. TAMBORENEA
TECHINT S. A., C. M. della Paolera 299, 1001 Buenos Aires, Argentina

(*Received* 12 *August* 1987 *and in final form* 5 *February* 1988)

**Abstract**—Plate heat exchanger arrangements, with a constant number of streams per pass for each fluid, and uniform fluid distribution, are classified in terms of five basic parameters. A program based on the diagonalization of a system of linear differential equations is constructed for the numerical calculation of the thermal effectiveness of an arbitrary arrangement. An alternative program is developed in the limit of a large number of plates. A comparative analysis of the results obtained is performed. Basic trends are discussed, and the early onset of asymptotic behaviour is pointed out.

## 1. INTRODUCTION

EVEN THOUGH plate heat exchangers (PHE) are becoming increasingly popular in various industrial applications, the literature on the subject of the calculation of the MTD or, equivalently, the thermal effectiveness of these arrangements, is rather limited [1–4]. Only very recently Shah and Kandlikar performed detailed calculations of single and multipass arrangements, in which the number of plates covers the practical range of applications [5, 6]. In the first paper they revised in detail the existing literature, and reported calculations of the effectiveness and MTD correction factor $F$ for configurations in which one fluid performs only one pass. In the second work, tabulations of similar results for the most common multipass geometries are given.

This paper is, in some sense, complementary to those of Shah and Kandlikar. Whereas they focused on the most common configurations, and wrote separate programs for the step-by-step integration of the differential equations for each of them, we use a different numerical approach to set up a scheme that can handle an arbitrary 'regular' geometry, and perform a comparative analysis of the various possible arrangements. As a necessary introductory task, we analyse in detail and classify all the geometries considered, the parameters that uniquely define them, and the occasional degeneracies that force the effectiveness of two apparently different configurations to be the same. We do find complete numerical agreement with the results tabulated in refs. [5, 6], in all cases examined.

Throughout this work we use the standard assumptions of temperature independence of the heat capacity rates and heat transfer coefficient, equality of the heat capacity rates for all the channels of each fluid, and negligible heat losses.

## 2. CLASSIFICATION OF ARRANGEMENTS

The number of possible PHE configurations is quite large. In order to classify them systematically, we consider the array of parallel plates, numbered from 1 to $N$, shown in Fig. 1, in which fluids 1 and 2 flow through $N+1$ adjacent channels.

Let $J$ and $K$ (with $J \leqslant K$) be the number of passes of the two fluids. When $J = K$, we call fluid 1 the fluid in channel 1. For $J < K$, fluid 1 is the fluid which performs $J$ passes. We restrict our analysis to regular configurations, in which the numbers $n_1$ and $n_2$ of channels per pass for each fluid are constant. As a consequence of this, and of the fact that fluids 1 and 2 alternate in neighbouring channels, there are limitations on the possible values of $N$, for given $J$ and $K$.

Let us examine first what odd values of $N$ are possible for given $J$ and $K$. If $N$ is odd, there is an even number of channels, and half of them are occupied by each fluid. Therefore, $(N+1)/2$ has to be simultaneously divisible by $J$ and $K$. Thus, the possible

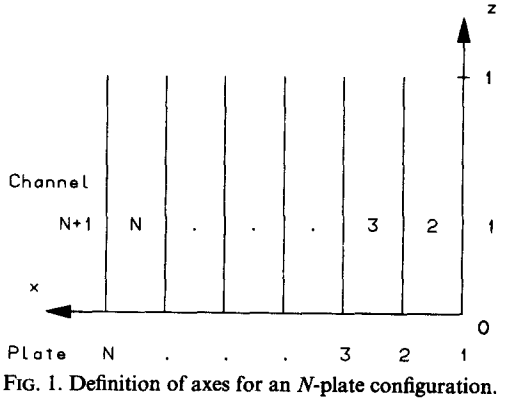


FIG. 1. Definition of axes for an $N$-plate configuration.

## NOMENCLATURE

| | |
|---|---|
| $A$ | heat transfer surface area [$m^2$] |
| $B$ | matrix relating the $\tau$ variables to stream temperatures [dimensionless] |
| $c$ | fluid 1 heat capacity rate [$J\,s^{-1}\,°C^{-1}$] |
| $C$ | fluid 2 heat capacity rate [$J\,s^{-1}\,°C^{-1}$] |
| $c_i$ | heat capacity rate of stream in the $i$th channel [$J\,s^{-1}\,°C^{-1}$] |
| $D$ | tridiagonal matrix which appears in the set of differential equations (7) [dimensionless] |
| $H$ | matrix which relates the stream temperatures at $z = 1$ to those at $z = 0$ |
| $J$ | number of passes of fluid 1 [dimensionless] |
| $K$ | number of passes of fluid 2 [dimensionless] |
| $m$ | largest common factor of $J$ and $K$ |
| $M$ | least common multiple of $J$ and $K$ |
| $N$ | number of thermal plates [dimensionless] |
| $n_1, n_2$ | number of channels per pass for fluids 1 and 2 [dimensionless] |
| $NTU$ | number of heat transfer units referred to fluid 1, $UA/c$ [dimensionless] |
| $P$ | fluid 1 thermal effectiveness, $(t'-t)/(T-t)$ [dimensionless] |
| $R$ | heat capacity rate ratio, $c/C$ [dimensionless] |
| $s_e, s_o$ | even- and odd-$\rho$-splittings, defined in equations (18) and (19) [dimensionless] |
| $U$ | overall heat transfer coefficient [$W\,m^{-2}\,°C^{-1}$] |
| $t, t'$ | inlet and outlet fluid 1 temperatures [°C] |
| $T, T'$ | inlet and outlet fluid 2 temperatures [°C] |
| $t_i$ | temperature of $i$th stream [°C] |
| $x$ | dimensionless coordinate normal to the plates |
| $z$ | dimensionless coordinate along the plates. |

Greek symbols

| | |
|---|---|
| $\Lambda$ | matrix resulting from the diagonalization of $D$ [dimensionless] |
| $\rho$ | relative flow parameter defined in Table 1 [dimensionless] |
| $\sigma$ | sequence parameter defined in Section 2 [dimensionless] |
| $\tau_i$ | linear combinations of the stream temperatures $t_i$ [°C] |
| $\phi$ | countercurrent fraction parameter defined in equation (20) [dimensionless]. |

odd values of $N$ are given by

$$N_i = 2iM - 1, \quad i = 1, 2, 3, \ldots \tag{1}$$

where $M$ is the least common multiple of $J$ and $K$. We say that an exchanger having a number of plates given by equation (1) belongs to the 'odd-$N$ sequence', and assign to it a sequence parameter $\sigma = 1$.

The analysis for even values of $N$ is somewhat more complicated, because two possibilities arise. In the first one we have

$$N = 2(n_1 J - 1) = 2n_2 K \tag{2}$$

and fluid 1 is found in channels 1 and $N+1$. These configurations belong to the 'fluid-1-outside' sequence, and are identified by $\sigma = 2$. Alternatively, we may have

$$N = 2n_1 J = 2(n_2 K - 1) \tag{3}$$

in which case fluid 1 is in channels 2 and $N$. These are 'fluid-1-inside' configurations, with $\sigma = 3$.

It can be proved that solutions of equations (2) and (3) with integer values of $n_1$, $n_2$, and $N$, exist if, and only if, the largest common factor $m$ of $J$ and $K$ is 1, i.e. if $M = JK$ [7]. In such cases, one solution with $N \leqslant 2JK$ can always be found. Given such a solution, additional ones are easily obtained with

$$n_1' = n_1 + iK$$
$$n_2' = n_2 + iJ, \quad i = 1, 2, 3, \ldots$$
$$N' = N + 2iJK$$

In summary, for given values of $J$ and $K$, we can identify three sequences of possible $N$ values, which increase in steps of $2M$. The sequences are called odd-$N$ ($\sigma = 1$), fluid-1-outside ($\sigma = 2$), and fluid-1-inside ($\sigma = 3$). The $\sigma = 1$ sequence is present for all values of $J$ and $K$. The even-$N$ sequences are present only for $J$ and $K$ such that $M = JK$, and they are distinct, i.e. they do not simultaneously occur for the same value of $N$, except for $J = K = 1$, in which case they coincide, and we need consider only the case $\sigma = 2$.

Each member of a sequence is therefore characterized by a set of compatible values of $J$, $K$, and $N$. There is often, however, more than one possible configuration for each of these sets of values, depending on the relative direction of flow of the fluids throughout the exchanger. In order to analyse these possibilities, we have to specify in detail the geometry of the arrangements considered.

For $J = K$ we have chosen to call fluid 1 the fluid in channel 1. For $J < K$ and $\sigma = 1$, fluid 1 is found either in channel 1 or $N+1$. In the latter case, if we renumber the plates backwards, calling plate 1 what was previously plate $N+1$, and vice versa, we find an

equivalent configuration in which fluid 1 is in channel 1. For $\sigma = 2$, we have already said that fluid 1 is necessarily in channel 1. Therefore, fluid 1 can always be assumed to be in channel 1, except in the $\sigma = 3$ configurations, in which case it is found in channel 2. In addition, we can assume that the fluid 1 stream in channel 1 or 2 is an inlet stream. Indeed, if it is an outlet stream, an equivalent configuration can be found using the property of flow reversibility, according to which the inversion of the direction of flow of both fluids does not alter the effectiveness of the arrangement [8].

Choosing as origin the end of plate 1 adjacent to the fluid 1 inlet, we draw a $z$-axis parallel to the direction of flow along the plates, and an $x$-axis normal to the plates, as shown in Fig. 1. With the conventions discussed above, the flow pattern of fluid 1 through the exchanger is then uniquely determined by the number of passes $J$ and the number of plates $N$. There are, however, four different possible paths for fluid 2, depending on the corner of the diagram of Fig. 1 near which the fluid 2 inlet is located. These four possible configurations for given $J$, $K$, and $N$, are characterized by two features:

(1) whether the overall connection is parallel-current or countercurrent (i.e. whether fluid 2, in proceeding from one pass to the following one, moves in the increasing $x$-direction, as fluid 1 does, or in the opposite one);

(2) whether the relative motion of fluids 1 and 2 along the first plate is, again, parallel-current or countercurrent.

We identify these four possible relative flow combinations by means of an integer relative flow parameter $\rho$. Table 1 shows the values assigned to $\rho$ for the four possible combinations of relative flow. An example of the four possible configurations for $(J, K) = (2, 5)$ and $N = 10$ is shown in Fig. 2.

These four cases do not always have different effectiveness. It is obvious that, if $J = 1$, i.e. if fluid 1 performs only one pass, the relative direction of flow of fluid 1 and fluid 2, in going from one pass to the next one, has no meaning. Therefore, the $\rho = 1$ and 4 cases coincide, and so do cases $\rho = 2$ and 3. Moreover, it is easy to verify that, if $N$ is even, and $(K-J)/m$ is odd, cases $\rho = 1$ and 3 are equivalent, and so are $\rho = 2$ and 4. In order to reach this conclusion, flow reversal, and renumbering of plates in inverse order, have again to be performed. In the example of Fig. 2 these transformations lead from $\rho = 1$ to 3, and from $\rho = 2$ to 4, and vice versa. In conclusion, Table 2 shows what are the equivalent $\rho$ values, and the multiplicity, i.e. the number of different configurations, for all the possible combinations of values of $N$, $J$, and $K$, including the limit $N \to \infty$. It should be noted that the multiplicity is the same for all $N$ values in a given sequence, because it depends only on $J$, $K$, and the evenness or oddness of $N$, which are common to all members of a sequence.

Table 1. Definition of the relative flow parameter $\rho$ for PHE

| $\rho$ | Overall relative flow | First plate relative flow |
|---|---|---|
| 1 | parallel-current | parallel-current |
| 2 | countercurrent | countercurrent |
| 3 | parallel-current | countercurrent |
| 4 | countercurrent | parallel-current |

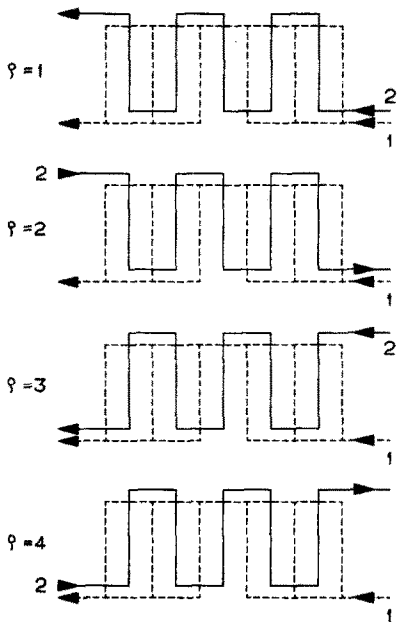


FIG. 2. Example of the four possible configurations, labeled $\rho = 1$–4, for a $(J, K) = (2, 5)$ exchanger with ten plates. In this case, the two odd-$\rho$ arrangements are equivalent, and the same is true for the even-$\rho$ geometries.

Table 2. Equivalent $\rho$ values and multiplicity for all possible combinations of $J$, $K$, and $N$

| $J$ | $(K-J)/m$ | $N$ | Equivalent $\rho$ values | Multiplicity |
|---|---|---|---|---|
| 1 | odd | $\infty$ | 1 = 4 = 2 = 3 | 1 |
| 1 | odd | even | 1 = 4 = 2 = 3 | 1 |
| 1 | odd | odd | 1 = 4, 2 = 3 | 2 |
| 1 | even | all | 1 = 4, 2 = 3 | 2 |
| >1 | odd | $\infty$ | 1 = 3, 2 = 4 | 2 |
| >1 | odd | even | 1 = 3, 2 = 4 | 2 |
| >1 | odd | odd | none | 4 |
| >1 | even | all | none | 4 |

## 3. DETERMINATION OF THE EFFECTIVENESS

We proceed in two steps in formulating and solving the differential equations which lead to the expression for the exchanger effectiveness. In the first stage, we write and diagonalize the equations for the $N+1$ channel temperature distributions, as functions of the dimensionless $z$-coordinate $(0 \leqslant z \leqslant 1)$, as if the streams were not connected to each other at the inlet and outlet ends of each channel. In the second stage, we introduce the connections as boundary conditions

of the solution. The effectiveness is then obtained by solving a linear system of algebraic equations.

The differential equations for the first and last stream temperatures are

$$c_1(\mathrm{d}t_1/\mathrm{d}z) = S_1(t_2 - t_1)UA/N \tag{4}$$

$$c_{N+1}(\mathrm{d}t_{N+1}/\mathrm{d}z) = S_{N+1}(t_N - t_{N+1})UA/N \tag{5}$$

whereas for the intermediate streams we write

$$c_i(\mathrm{d}t_i/\mathrm{d}z) = S_i(t_{i-1} + t_{i+1} - 2t_i)UA/N, \quad i = 2, \ldots, N. \tag{6}$$

In the equations above, $S_i$ is either 1 or $-1$, depending on whether the $i$th stream flows in the direction of increasing or decreasing values of $z$. In matrix notation, the equations can be written as

$$(N/NTU)[\mathrm{d}t(z)/\mathrm{d}z] = Dt(z) \tag{7}$$

where $t(z)$ is a vector of components $t_1(z)$, $t_2(z), \ldots, t_{N+1}(z)$, and $D$ is a tridiagonal matrix, because equations (4)–(6) only couple each unknown temperature to the neighbouring ones. Matrix equation (7) can be solved through a similarity transformation which diagonalizes $D$. Introducing the auxiliary temperature distributions $\tau_i(z)$, such that

$$t_i(z) = \sum_j B_{ij}\tau_j(z) \tag{8}$$

we substitute into equation (7) and obtain, using matrix notation

$$(N/NTU)\,\mathrm{d}\tau/\mathrm{d}z = B^{-1}DB\tau(z) = \Lambda\tau(z). \tag{9}$$

We choose matrix $B$ such that $\Lambda$ is diagonal, and from the relation

$$DB = B\Lambda \tag{10}$$

we verify that $b_i$, the $i$th column of $B$, is an eigenvector of $D$ with an eigenvalue equal to the $i$th diagonal element of matrix $\Lambda$. After obtaining the eigenvalues and eigenvectors through standard numerical techniques, the solution of equation (9) can be written as

$$\tau(z) = \exp(NTU\,\Lambda z/N)\tau(0). \tag{11}$$

For the temperature variables at $z = 1$ we obtain

$$t(1) = Ht(0) \tag{12}$$

with

$$H = B\exp(NTU\,\Lambda/N)B^{-1}. \tag{13}$$

Equation (12) is actually a set of $N+1$ algebraic equations relating the $N+1$ temperatures at $z = 1$ to the corresponding ones at $z = 0$. These equations have to be complemented by the specification of the inlet temperatures of the two fluids in their respective first passes, and additional equations stating that the inlet temperature for each stream of subsequent passes is the average of the outlet temperatures of the preceding pass. After elimination of all the intermediate temperatures, we are left with a linear relation for the outlet fluid 1 temperature as a function of the inlet ones for fluids 1 and 2. The effectiveness $P$ is then obtained from

$$P = (t' - t)/(T - t). \tag{14}$$

## 4. ASYMPTOTIC CALCULATIONS

Consider a countercurrent exchanger with $J = K = 1$ and $N$ plates. Streams 1 and $N+1$ exchange heat with only one neighbouring stream, whereas each one of the other streams exchanges heat with two neighbours. This gives rise to 'end effects' which cause the temperature distributions of the first and last streams to differ from those of the middle streams. These effects propagate to a few streams away from the ends of the exchanger, and are responsible for the deviation of the exchanger effectiveness from that of a purely counterflow configuration. As the number of plates increases, the influence of these end effects tends to disappear, as discussed by Shah and Kandlikar for $J = 1$ [5].

Similar effects are found in multipass exchangers in the vicinity of the boundaries between consecutive passes of either fluid, and, again, for given $J$ and $K$, disappear in the limit $N \to \infty$. In this asymptotic limit, the exchanger can be reduced to an assembly of components which are purely parallel or countercurrent exchangers.

Consider, for example, a $J = 4$, $K = 6$, $\rho = 1$ exchanger. Figure 3(a) shows the flow pattern of the two fluids, with indication of the pass boundaries. Not counting both ends of the exchanger, there are $J-1 = 3$ boundaries for fluid 1, and $K-1 = 5$ ones for fluid 2. Actually, because $J$ and $K$ are both multiples of 2, in the middle of the exchanger we find a double boundary, where pass boundaries for both fluids coincide. In general, there are $m-1$ such double boundaries, which divide the exchanger into $m$ 'prime segments'. Each of these segments has one inlet and one outlet stream for either fluid, and is coupled to the neighbouring segments. Depending on the evenness or oddness of the relative flow parameter $\rho$, this coupling is of the countercurrent series or cocurrent series type. The effectiveness of the whole exchanger can be obtained in terms of the effectiveness of the segments through well-known coupling formulae [9]

$$P = \left\{1 - \prod_{i=1}^{m}[1 - (1+R)P_i]\right\} \Big/ (1+R) \tag{15}$$

for cocurrent series coupling, and

$$P = \left[\prod_{i=1}^{m}(1 - RP_i) - \prod_{i=1}^{m}(1 - P_i)\right] \Big/ \left[\prod_{i=1}^{m}(1 - RP_i) - R\prod_{i=1}^{m}(1 - P_i)\right] \tag{16}$$

for coupling of the countercurrent series type. For $R = 1$, equation (16) is substituted by

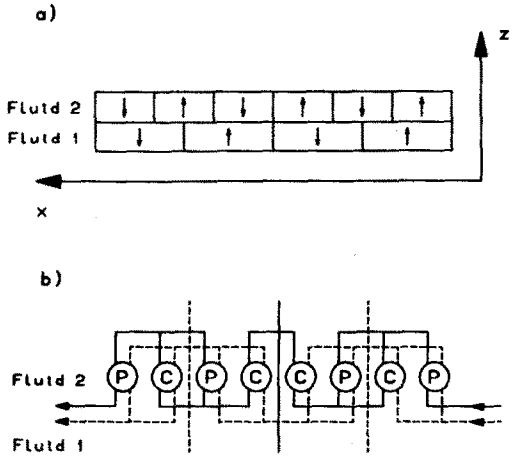


FIG. 3. (a) Flow pattern of a $(J, K) = (4, 6)$ exchanger with $\rho = 1$, in the limit of large $N$. (b) Decomposition of the same exchanger into two prime segments, each consisting of two parts which, in turn, are split into parallel-current (P) and countercurrent (C) components.

$$P = \left[\sum_{i=1}^{m} P_i/(1-P_i)\right] \Big/ \left[1 + \sum_{i=1}^{m} P_i/(1-P_i)\right]. \quad (17)$$

Observe, however, that each prime segment is an exchanger with the same heat capacity rate ratio of the overall exchanger, but a number of heat transfer units $m$ times smaller.

The determination of the effectiveness of each prime segment is performed by decomposing it into parts delimited by the fluid 1 boundaries. In Fig. 3(b) these boundaries within a segment are shown by vertical dashed lines. In the most general case, each of the component parts has one inlet and one outlet stream for fluid 1, but two inlet and two outlet streams for fluid 2. Thus, a generalized matrix formalism with $3 \times 3$ matrices has to be used for the description of each part, and for coupling these parts to each other [10]. Each part is in turn constituted by pure parallel-current or countercurrent components, plus nodes at which two streams merge into one, or one is divided into two. In the example of Fig. 3, the $J = 4$, $K = 6$, $\rho = 1$ exchanger is split into two prime segments, each segment into two parts, and each part into two components. Such a reduction, with a variable number of constituents at each stage, can be done in the most general case, and was implemented into a computer program that performs it for arbitrary $J$, $K$ and $\rho$, and provides the asymptotic value of the effectiveness in the limit of a large number of plates.

## 5. RESULTS AND DISCUSSION

The classification of PHE discussed in Section 2 shows that a configuration is uniquely specified by the variables $R$ and $NTU$, and the parameters $J$, $K$, $N$, and $\rho$. In addition, it can be identified as belonging to one of three distinct sequences, labeled by the parameter $\sigma$. We attempt here to establish the basic trends observed for the effectiveness as we scan these possible configurations.

In the following, we often compare the effectiveness of two or more arrangements, for the same values of $R$ and $NTU$, and different geometries. We know that changes in the geometry, such as in the number of passes, may alter the fluid velocities, and, therefore, the heat transfer coefficient and $NTU$. Such indirect consequences of changes in the geometry are not taken into account in the present analysis, and should be incorporated separately by the designer.

Even though the dependence on the variables and parameters are intertwined, we single out the following trends.

1. Dependence on the relative-flow parameter $\rho$.

Figure 4 shows plots of $P$ vs $NTU$ at fixed $R$ for $\rho = 1$–4, for approximately 15 plates, and the following $(J, K)$ configurations: (2, 2), (2, 3), (2, 4), (3, 3), and (4, 4). For a comparative analysis of these curves it is convenient to define the 'even-$\rho$-splitting'

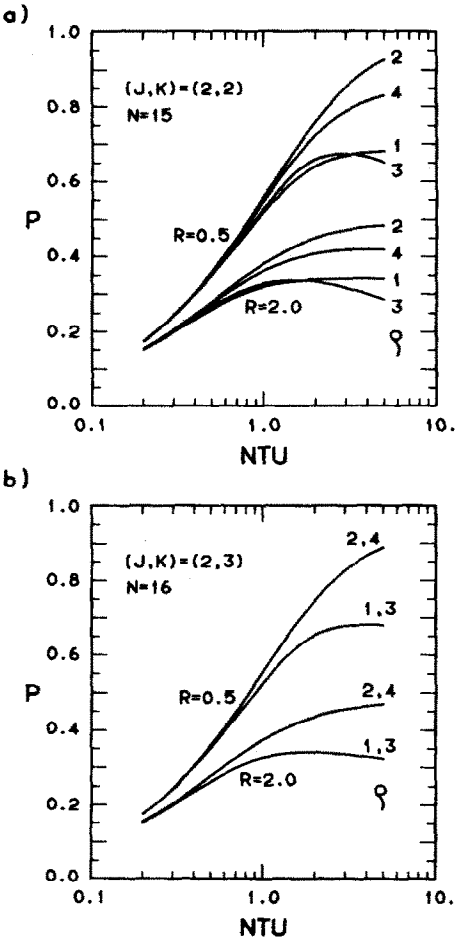


FIG. 4. Effectiveness $P$ as a function of $NTU$ for $R = 0.5$ and 2.0, for all four possible values of the relative flow parameter $\rho$ and: (a) $(J, K) = (2, 2)$, $N = 15$; (b) $(J, K) = (2, 3)$, $N = 16$; (c) $(J, K) = (2, 4)$, $N = 15$; (d) $(J, K) = (3, 3)$, $N = 17$; (e) $(J, K) = (4, 4)$, $N = 15$.

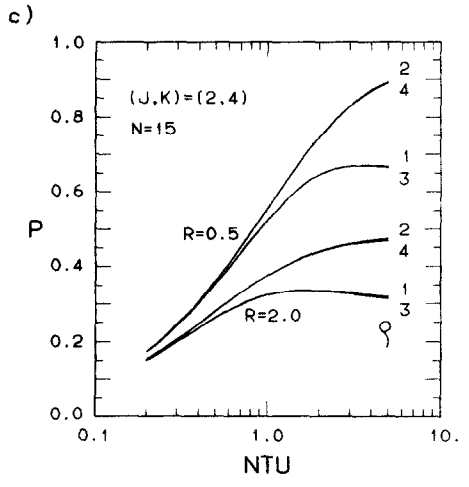


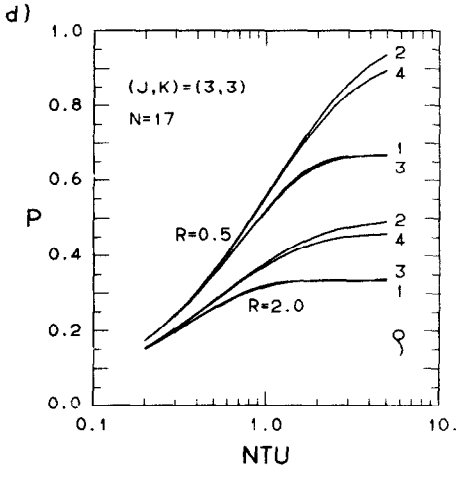


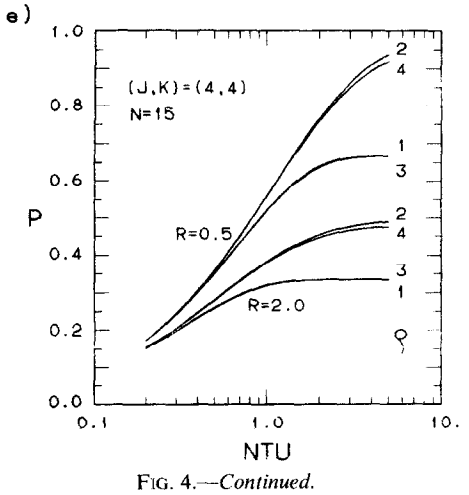


FIG. 4.—*Continued.*

$$s_e = P(\rho = 2) - P(\rho = 4) \tag{18}$$

and the analogous 'odd-$\rho$-splitting'

$$s_o = P(\rho = 3) - P(\rho = 1). \tag{19}$$

We summarize our observations as follows.

1.1. Even values of $\rho$ systematically give rise to higher effectiveness than odd $\rho$ values.

1.2. The even- and odd-$\rho$-splittings vanish for $(J, K) = (2, 3)$ and $N = 16$.

1.3. In the (2, 4) case both splittings are quite small.

1.4. The splittings for the $J = K$ configurations (2, 2), (3, 3), and (4, 4) decrease as $J$ increases.

1.5. $s_e$ is always positive in the examples shown.

1.6. $s_o$ is positive for low values of $NTU$, but, as $NTU$ increases, it changes sign.

We proceed now to discuss these observations. In the first place, for $J > 1$ it is natural to expect that overall countercurrent flow (i.e. even values of $\rho$), gives rise to higher effectiveness than overall parallel flow, and this is consistent with observation 1.1 above.

Observation 1.2 is immediately understood from examination of Table 2, which shows that, when $N$ is even and $(K-J)/m$ is odd, both splittings should vanish.

The smallness of the splittings pointed out in observation 1.3 is due to the fact that the $(J, K) = (2, 4)$ configuration has also an odd value of $(K-J)/m$, and, therefore, the $\rho$-splittings are forced to vanish in the limit of large $N$ (Table 2). What should be remarked is that this asymptotic trend is already visible at $N = 15$.

Observation 1.4 can be understood from the fact that, for $K = J$, as $J$ increases, for any given value of $NTU$, even-$\rho$ configurations approach the pure countercurrent geometry, and odd-$\rho$ ones approach parallel flow. Again, it is remarkable that this large-$J$ trend is visible at such low values of $J$.

In order to analyse the sign of $s_e$ and $s_o$, it is useful to introduce into the analysis the countercurrent fraction parameter $\phi$ defined as

$$\phi = \text{Number of countercurrent plates}/N. \tag{20}$$

The numerator of this fraction is the number of plates for which the adjacent fluid streams flow in opposite directions. For any given configuration, the parameter $\phi$ is easily computed by inspection, and for the asymptotic $N \to \infty$ limit we find

$$\begin{aligned}
&\phi(J, K) = 1/2, && \text{for odd } (K-J)/m \\
&\phi(J, K) = 1/2 + m^2/2JK, && \text{for even } (K-J)/m,\ \rho = 2, 3 \\
&\phi(J, K) = 1/2 - m^2/2JK, && \text{for even } (K-J)/m,\ \rho = 1, 4.
\end{aligned} \tag{21}$$

It is reasonable to expect that, for the same values of $J$ and $K$, and the same overall relative flow, the configurations with higher $\phi$ should have higher effectiveness. Comment 1.5 is consistent with this expectation, and we found instances in which $s_e$ is negative with larger $\phi$ values for $\rho = 4$ than for $\rho = 2$. Observation 1.6 also confirms the $\phi$ dominance for low $NTU$ values. The change of sign at large $NTU$ is explained by the following line of reasoning.

Consider, for simplicity, the asymptotic model for

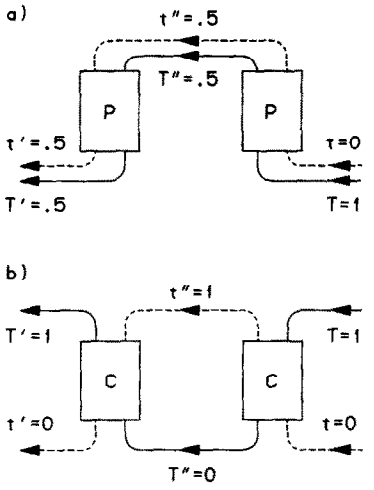


FIG. 5. Block diagram for the $(J, K) = (2, 2)$, overall parallel-current configurations, in the limit of large $N$ and $NTU$: (a) for $\rho = 1$; (b) for $\rho = 3$.

$(J, K) = (2, 2)$, and overall parallel flow (odd $\rho$). In this limit, the exchanger can be decomposed into two prime segments of either parallel-current or counter-current type, depending on whether we have $\rho = 1$ or 3, respectively, as shown in Fig. 5. For small $NTU$, the $\rho = 3$ case, with $\phi = 1$, is more effective than the $\rho = 1$ case, with $\phi = 0$, as expected. As $NTU$ increases, however, the $\rho = 3$ case approaches the point in which the cold fluid outlet of the first stage is warmer than the first stage hot fluid outlet. When this happens, reverse heat transfer occurs in the second stage of the exchanger, and this conspires against the overall effectiveness. In the limit of $NTU \to \infty$, we find, for $R = 1$, the extreme result indicated in Fig. 5(b), in which the second stage completely neutralizes the effect of the first one, and the overall effectiveness is zero. On the other hand, we observe that, in this limit, the $\rho = 1$ case of Fig. 5(a) leads to the same outlet temperatures for both fluids and, therefore, $P(\rho = 1) = 0.5$. This demonstrates how degradation due to reverse heat transfer may give rise to negative values of $s_0$ at large $NTU$.

2. Dependence on the number of plates.

Figure 6 shows the $N$-dependence of the effectiveness for some (2, 3) arrangements, which we take as illustrations of trends that can also be found in other geometries. The main features observed from these plots, and similar ones that we do not have enough space to reproduce here, are given below.

2.1. As expected, the effectiveness for different $\sigma$ sequences approaches the same limiting value, as $N \to \infty$.

2.2. The $N$ dependence of the effectiveness for each $\sigma$ sequence is smooth. If, however, we do not classify the geometries with the $\sigma$ parameter, and consider simultaneously all possible $N$ values for given $J$, $K$, and $\rho$, the effectiveness oscillates as a function of $N$.

2.3. The differences between the effectiveness of

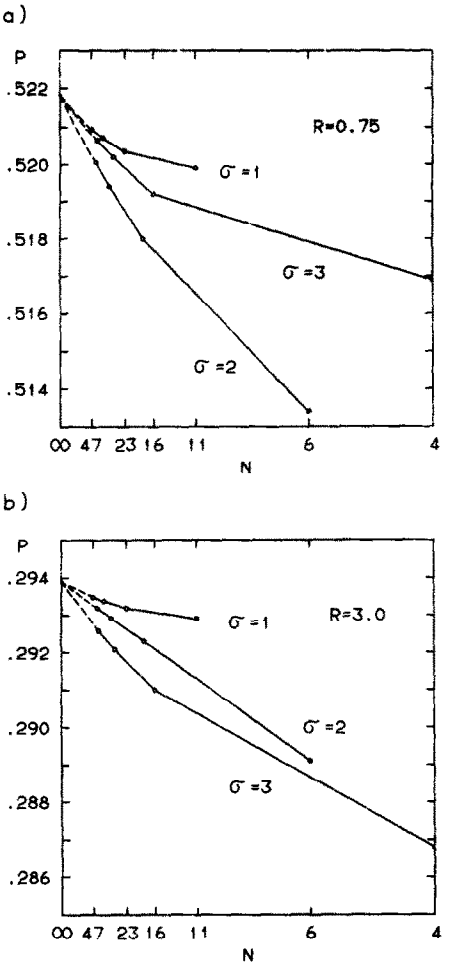


FIG. 6. Effectiveness as a function of the number of plates $N$, using a $1/N$ scale, for $(J, K) = (2, 3)$, $\rho = 2$, $NTU = 1$: (a) $R = 0.75$; (b) $R = 3.0$. Values belonging to the same $\sigma$-sequences are connected by straight lines. The last calculated point is connected by a dashed line to the asymptotic limit.

sequences of the same $J$, $K$, and $\rho$, but different $\sigma$, are usually small, and depend mainly on $\phi$ and $R$. Higher effectiveness tends to be associated with larger values of $\phi$, and this is responsible for the larger values of $P$ for $\sigma = 1$ in Fig. 6. In addition, values of $R$ larger than $K/J$ tend to favour $\sigma = 2$ and depress $\sigma = 3$, whereas the opposite is true for $R < K/J$.

2.4. The slope of the plots of Fig. 6 at $1/N = 0$ measures the rate at which the asymptotic limit is approached. The larger the slope is, the larger the value of $N$ required to approach the asymptotic limit within a given accuracy. In the examples of Fig. 6, this limit is approached within 1% for $N \geqslant 16$.

2.5. Because deviations from the asymptotic limit are due to end effects, and, as $J$ and $K$ increase, more pass boundaries are present, we might expect the slope at $1/N = 0$ to increase for larger values of $J$ and $K$. This is not seen to happen in practice, which may be interpreted as an indication that end effects do not tend to add coherently but, rather, to partially cancel each other.

## 6. VARIABLE PROPERTIES AND COEFFICIENTS

As stated in the Introduction, throughout this work the heat capacity rates and heat transfer coefficient have been assumed to be constant. If this restriction is released, the mathematical nature of the problem changes in a fundamental way. Because the coefficients of the differential equations (4)–(6) are functions of the temperature, the problem ceases to be linear, and requires an entirely numerical solution.

Within the present scheme it is possible, however, to account in an approximate way for this temperature dependence, both in the case of a finite number of plates, and in the large-$N$ limit, with the following iterative procedure. As a first approximation, an initial guess is taken for the temperature-dependent parameters, which may, for instance, be assigned the values corresponding to the inlet temperatures. After the calculation is performed, and the temperatures of all streams are known throughout the exchanger, an adequate average value is assigned to the parameters for each one of the streams, and the process is iterated until convergence is achieved.

## 7. CONCLUSION

We have systematically classified the possible PHE configurations, and shown two methods for solving the thermal problem. One is based on the numerical solution of the 'exact' equations and, as the number of plates increases, it becomes more demanding in computer time, memory and precision. The other method is valid in the limit of a large number of plates, and is extremely fast. In practice, both methods complement each other, and when the former becomes too cumbersome, the latter is sufficiently accurate for practical applications.

The trends observed in the analysis of the results obtained provide the basis for a qualitative understanding of the mechanisms involved. What is probably the most important feature detected is the early approach of asymptotic behaviour, whereby results expected to hold in the large-$J$ or large-$N$ limits, are found to set in at fairly low values of these parameters.

*Acknowledgements*—The authors are indebted to Guillermo Marshall of CNEA, Guillermo Cordero of TECHINT, and Eduardo Dvorkin of SIDERCA for enlightening discussions of different aspects of this work. This work was supported in part by a CONICET-NSF Cooperative Science Program.

## REFERENCES

1. B. W. Jackson and R. A. Troupe, Plate exchanger design by the $\varepsilon$–$NTU$ method, *Chem. Engng Prog. Symp. Ser. No.* 64 **62,** 185–190 (1966).
2. M. R. Foote, Effective mean temperature differences in multipass heat exchangers, NEL Report 303, National Engineering Laboratory, Glasgow, U.K. (1967).
3. J. D. Usher, The plate heat exchanger. In *Compact Heat Exchangers*, NEL Report 482, National Engineering Laboratory, Glasgow, U.K. (1969).
4. S. G. Kandlikar, Performance curves for different plate heat exchanger configurations, ASME Paper No. 84-HT-26 (1984).
5. R. K. Shah and S. G. Kandlikar, The influence of the number of thermal plates on plate heat exchanger performance. In *Current Researches in Heat and Mass Transfer*, pp. 267–288. Hemisphere, Washington, DC (1988).
6. R. K. Shah and S. G. Kandlikar, Multipass plate heat exchangers—effectiveness—$NTU$ results and guidelines for selecting pass arrangements, *ASME J. Heat Transfer*, to be published.
7. G. H. Hardy and E. M. Wright, *An Introduction to the Theory of Numbers*, 4th Edn, Chap. V, Theorem 57. Clarendon Press, Oxford (1960).
8. A. Pignotti, Flow reversibility of heat exchangers, *ASME J. Heat Transfer* **106,** 361–368 (1984).
9. J. D. Domingos, Analysis of complex assemblies of heat exchangers, *Int. J. Heat Mass Transfer* **12,** 537–548 (1969).
10. A. Pignotti, Matrix formalism for complex heat exchangers, *ASME J. Heat Transfer* **106,** 352–360 (1984).

## EFFICACITE THERMIQUE DES ECHANGEURS A PLAQUES MULTIPASSES

**Résumé**—Les arrangements d'échangeur à plaques, avec un nombre constant de courant par passe pour chaque fluide et une distribution uniforme de fluide, sont classés en fonction de cinq paramètres fondamentaux. Un programme basé sur la diagonalisation d'un système, d'équations différentielles linéaires est construit pour le calcul numérique de l'efficacité thermique d'un arrangement arbitraire. Un programme alternatif est développé dans la limite d'un grand nombre de plaques. Une analyse comparative des résultats est conduite. On discute les tendances de base et on dégage le comportement asymptotique déjà connu.

## THERMISCHER WIRKUNGSGRAD VON MEHRGÄNGIGEN PLATTENWÄRMETAUSCHERN

**Zusammenfassung**—Anordnungen von Plattenwärmetauschern mit einer konstanten Zahl von Strömen pro Pfad für jedes Fluid und gleichmäßiger Verteilung werden mit Hilfe von fünf Grund-Parametern eingeteilt. Ein Programm, das auf der Diagonalisierung eines Systems linearer Differentialgleichungen beruht, wird zur numerischen Berechnung des thermischen Wirkungsgrades einer beliebigen Anordnung erstellt. Ein Alternativprogramm wird für eine große Anzahl von Platten entwickelt. Eine vergleichende Analyse der erhaltenen Ergebnisse wird durchgeführt. Grundlegende Trends werden diskutiert und das frühe Einsetzen des asymptotischen Verhaltens wird herausgearbeitet.

## ТЕПЛОВАЯ ЭФФЕКТИВНОСТЬ МНОГОХОДОВЫХ ПЛАСТИНЧАТЫХ ТЕПЛООБМЕННИКОВ

**Аннотация**—Пластинчатые теплообменники с постоянным числом каналов для каждой жидкости и однородным ее распределением классифицируются на основе пяти основных параметров. Для численного расчета тепловой эффективности произвольного теплообменника создана программа, основанная на диагонализации системы линейных дифференциальных уравнений. Создан вариант программы для предельно большого числа пластин. Проведен сравнительный анализ полученных результатов. Обсуждаются основные тенденции и отмечено более раннее проявление асимптотического поведения.